

RESEARCH ARTICLE OPEN ACCESS

Drivers of Spatiotemporal Patterns of Riparian Forest NDVI Along a Hydroclimatic Gradient

Pierre Lochin¹  | Hervé Piégay¹  | John C. Stella²  | Kelly K. Caylor^{3,4,5}  | Lise Vaudor¹ | Michael Bliss Singer^{3,6,7} 

¹ENS de Lyon, UMR 5600 Environnement Ville société, CNRS, Lyon, France | ²Department of Sustainable Resources Management, State University of New York College of Environmental Science and Forestry, Syracuse, New York, USA | ³Earth Research Institute, University of California, Santa Barbara, California, USA | ⁴Department of Geography, University of California, Santa Barbara, Santa Barbara, California, USA | ⁵Bren School of Environmental Science & Management, University of California, Santa Barbara, California, USA | ⁶Water Research Institute, Cardiff University, Cardiff, UK | ⁷School of Earth and Environmental Sciences, Cardiff University, Cardiff, UK

Correspondence: Pierre Lochin (pierre.lochin@ens-lyon.fr)

Received: 8 December 2023 | **Revised:** 11 September 2024 | **Accepted:** 3 October 2024

Funding: This work was supported by the Graduate School H2O'Lyon (ANR-17-EURE-0018) of Université de Lyon (UdL), within the program “Investissements d'Avenir” operated by the French National Research Agency (ANR), by the National Science Foundation (EAR 1700517, EAR 1700555 and BCS 1660490) and by the US Department of Defense's Strategic Environmental Research and Development Program-SERDP (RC18-1006).

Keywords: greenness | remote sensing | Rhône | Sentinel-2 | vegetation

ABSTRACT

In the context of rising global temperatures and their impact on weather patterns and water cycles, understanding the relationship between vegetation and hydroclimatic forcing is critical. Riparian forests are highly vulnerable to hydroclimatic variability, which can significantly affect water availability in the soil on which they primarily depend. Along large rivers, hydroclimatic forcings can vary, resulting in different vegetative responses depending on the local climatic context and site conditions. To explore this, we studied riparian forest greenness along a 512-km river corridor with a 3° latitudinal gradient, analysing the relative contributions of climate (latitude, season, temperature, precipitation) and local hydrological conditions (groundwater). Here, we show that riparian forests along a latitudinal gradient respond differently to hydroclimatic controls, with vegetative dynamics that can be attenuated or accentuated by local site conditions. We combined Sentinel-2 satellite Normalised Difference Vegetation Index (NDVI) data over seven years (2016–2022) with hydroclimatic data to examine riparian forest greenness responses to latitudinal, seasonal and interannual hydroclimatic variability. We found contrasting hydroclimatic controls across the latitudinal gradient, with the northernmost sites predominantly controlled by temperature, while those further south are limited by water availability. In addition, we identified temperature as the primary driver of NDVI throughout the growing season, either positively or negatively. Late season precipitation and high phreatic water availability positively influenced NDVI, emphasising the role of local conditions in governing riparian forest resilience. This study enhances understanding of climate controls on riparian tree greenness, which is critical for designing effective landscape-scale riparian ecosystem management and restoration strategies.

1 | Introduction

Forests worldwide are becoming increasingly vulnerable to climate forcing, particularly because of increasing water stress (Allen, Breshears, and McDowell 2015; Choat et al. 2012; Peters

et al. 2021). Despite their location in riverine corridors, riparian forests are not exempt from water stress constraints; on the contrary, they are highly sensitive to both local and regional climate controls on water availability (Kibler et al. 2021; Pettit and Froend 2018; Rohde et al. 2021; Williams et al. 2022). Local

This is an open access article under the terms of the [Creative Commons Attribution-NonCommercial-NoDerivs License](#), which permits use and distribution in any medium, provided the original work is properly cited, the use is non-commercial and no modifications or adaptations are made.

© 2024 The Author(s). *Ecohydrology* published by John Wiley & Sons Ltd.

climate variability plays a crucial role in controlling water availability in the root zone, by regulating soil-atmosphere exchange (Berg and Sheffield 2018; Seneviratne et al. 2010). During the growing season, an increase in temperature and a decrease in precipitation lead to elevated atmospheric water demand and higher rates of evapotranspiration, depleting soil moisture. Reduced water availability can be further exacerbated by decreased phreatic zone water availability due to declining streamflow (Evans, Dritschel, and Singer 2018; Rivaes et al. 2013). Riparian tree species are vulnerable to declines in water availability because they often rely on access to vadose (unsaturated) or phreatic (saturated) zone water resources for survival (Singer et al. 2013; Stella and Battles 2010). Consequently, during dry periods, most riparian trees close their stomata to cope with water stress (Hultine et al. 2020; McDowell et al. 2008). While this behaviour aids in short-term water stress management, it can have long-term consequences, such as leaf abscission or branch dieback, which affect the overall growth, health and productivity of riparian trees (Kibler et al. 2021; Scott, Shafrroth, and Auble 1999; Stella et al. 2013).

However, reductions in water availability and increased atmospheric water demand do not affect all riparian forests uniformly. Different riparian species use varying water sources due to their rooting systems (Rood, Bigelow, and Hall 2011), resulting in unequal susceptibility to water stress (Sargeant and Singer 2016; 2021; Singer et al. 2014). Likewise, the magnitude of climate controls on water availability varies depending on the local climatic context (Palmer et al. 2008), especially along large rivers within basins characterised by significant hydroclimatic variability (Puckridge et al. 1998), resulting in different responses of riparian forests to climate forcing (Mayes et al. 2020; Sargeant and Singer 2021). In temperate climates with wet summers, the risk of vadose zone drying is limited, as evapotranspiration rarely exceeds precipitation. Conversely, in arid or semi-arid climates, the balance between evapotranspiration and precipitation can shift rapidly. In Mediterranean-climate regions, riparian ecosystems are considered resource-rich “islands” due to their ecological importance relative to the proportion of land area they occupy (Stella et al. 2013). At the same time, Mediterranean riparian ecosystems are highly vulnerable to anthropogenic pressures, particularly on water resources (Merritt et al. 2010; Tonkin et al. 2018). The impact of climate change on precipitation and streamflow patterns intensifies these pressures, disrupting the balance between evapotranspiration and precipitation and ultimately leading to a reduction in water availability (Giorgi and Lionello 2008; Lionello et al. 2006). In this context, the conservation and restoration of riparian forests will become more challenging in the coming decades.

There is a growing consensus that riparian ecosystems are likely to play a significant role in enabling natural and human systems to adapt to climate change (Capon et al. 2013; Palmer et al. 2008; Seavy et al. 2009). Indeed, riparian forests act as biodiversity hot spots and provide a variety of ecosystem services ranging from ecological conservation and biodiversity to cultural values and recreation (Matzek, Stella, and Ropion 2018; Riis et al. 2020). Characterising the climate factors that control water availability in riparian forests at different temporal and spatial scales is essential to anticipate the responses of these

ecosystems to future climate change (Capon et al. 2013; Seavy et al. 2009). To achieve this, it is necessary to gain a comprehensive understanding of the influence of climate control on riparian greenness at spatial and temporal scales that incorporate climatic variability, as well as seasonal and interannual variability. Several studies have emphasised the importance of expanding study scales to incorporate climate variability that can affect riparian zones within the same watershed (Capon et al. 2013; González et al. 2017; Seavy et al. 2009). However, few studies have focused on the effects of a hydroclimatic gradient on climate controls on water availability in riparian forests. Some recent studies, however, have shown that riparian greenness responses can fluctuate on broader spatial scales (Pace et al. 2021; Rohde et al. 2021). Improving our understanding of hydroclimatic controls on riparian tree greenness in the recent past will help us better predict how riparian trees will respond to climate change in the coming years. A better understanding of climate controls in the warmest and driest areas along large rivers may provide clues to what we can expect to see as more widespread responses as climate change unfolds in colder and wetter areas.

Until recently, studying riparian vegetation at large scales has been challenging due to the fragmentation of riparian forests and the need for significant human and financial resources to monitor them along long corridors with significant changes in hydroclimatic forcing. Remote sensing tools have facilitated the study of riparian ecosystems by providing continuous data at various spatial scales (Carboneau and Piégay 2012; Piégay et al. 2020). High-resolution imagery from airborne sensors has allowed for the study of riparian dynamics at finer scales locally (Huylenbroeck et al. 2020), whereas satellite imagery provides data at larger scales but with limited spatial resolution (Henshaw et al. 2013). The launch of the Sentinel satellites in 2016 has provided a good compromise between spatial resolution and large-scale coverage, providing relatively high temporal resolution to explore intra-annual/seasonal patterns. Already widely used for assessing riparian vegetation, Sentinel data have proven valuable for characterising vegetation variation and change at finer scales (Rohde et al. 2021; Romano, Ricci, and Gentile 2020). Furthermore, remote sensing provides an avenue for evaluating greenness through metrics such as the normalised difference vegetation index (NDVI). Higher NDVI values correspond to increased photosynthetic activity and canopy density (Bannari et al. 1995; Huang et al. 2021). This index is frequently employed as an indicator of vegetation health and is commonly used to analyse riparian vegetation variation and change at the landscape scale (Daryaei et al. 2020; Sabathier et al. 2021). NDVI has been widely used to study the relationships with hydroclimatic variables (Fu and Burgher 2015; Wang, Rich, and Price 2003). Finally, remote sensing can be used to retrospectively analyse the responses of riparian forests to climate controls at large spatial scales, allowing for consideration of the entire river corridor.

In this study, we analyse the spatiotemporal variability of riparian tree greenness (NDVI) using high temporal resolution Sentinel-2 data to better characterise riparian forest responses to hydroclimatic drivers along a 3° latitudinal gradient spanning 500 km and temperate to semi-arid climates. We hypothesise that riparian forest greenness is influenced

by climate-related factors (temperature and precipitation) that vary over time (seasons and years) and space (latitude) and that the negative impacts of drought can be mitigated if groundwater is accessible. We design a specific framework to test our hypothesis by (1) exploring the seasonal and interannual variability of NDVI along the latitudinal gradient and its relationship with hydroclimatic variables, (2) assessing the contribution and influence of climate variables on NDVI at different periods of the growing season through model comparison and (3) analysing the influence of groundwater on NDVI at different temporal scales.

2 | Methods

2.1 | Study Area

Our study examines the riparian forest corridor along the French portion of the Rhône River, which spans 512 km between Geneva and the Mediterranean Sea (Olivier et al. 2022). The Rhône is a major European river with a catchment area of 90,500 km² and a mean annual discharge of 1700 m³ s⁻¹, primarily driven by snowmelt from alpine branches and also by precipitation, which can generate winter, spring or autumnal floods on its northern and alpine tributaries (Petts 1989; Vivian 1989). The Rhône River is mainly oriented north-south (Figure 1a) and follows a latitudinal gradient (3° between 46° and 43° north) that controls temperature and precipitation. This specific configuration makes it particularly suitable for investigating the response of riparian forests to changes in hydroclimatic conditions. Indeed, the southern sections of the Rhône are influenced by a Mediterranean climate. Summers are dry and hot, with precipitation occurring in spring and

fall. The upper part of the Rhône typically experiences cooler and wetter summers (Olivier et al. 2022; Sauquet et al. 2019). Over the growing season, a pronounced linear climate gradient was observed from Geneva to Avignon, with temperatures increasing by approximately 1.4°C per degree of latitude (Figure 1b) and precipitation decreasing by 103 mm per degree of latitude (Figure 1c). In the early 20th century, declines in grazing and agriculture facilitated the expansion of Rhône riparian forests into the fine-grained soils of the floodplain. In the last century, channel training to promote navigation and the development of hydroelectric dams and canals resulted in significant changes in hydrological connectivity due to channel incision and bypass channels (Seignemartin et al. 2023), which significantly reduced overbank flooding, water table levels and channel mobility. Consequently, vegetation dynamic processes, such as disturbance, succession and recruitment, were severely curtailed, leading to less age variation and greater age of extant forest stands, as well as composition shifts (Pautou, Girel, and Borel 1992). As a result, pioneer species, such as *Populus nigra* and *Salix alba*, have declined significantly and have been replaced by postpioneer and shade-tolerant species such as *Fraxinus excelsior* and the non-native and invasive *Acer negundo* and *Robinia pseudoacacia* (Janssen et al. 2020; Räpple 2018). Today, the dominant riparian tree species include *Populus nigra*, *Populus alba*, *Fraxinus excelsior*, *Fraxinus angustifolia*, *Salix alba*, *Alnus glutinosa*, *Acer negundo* and *Robinia pseudoacacia* (Olivier et al. 2022).

2.2 | Study Sites

We identified potential riparian forest sites using remote sensing data from aerial photographs provided by the French National

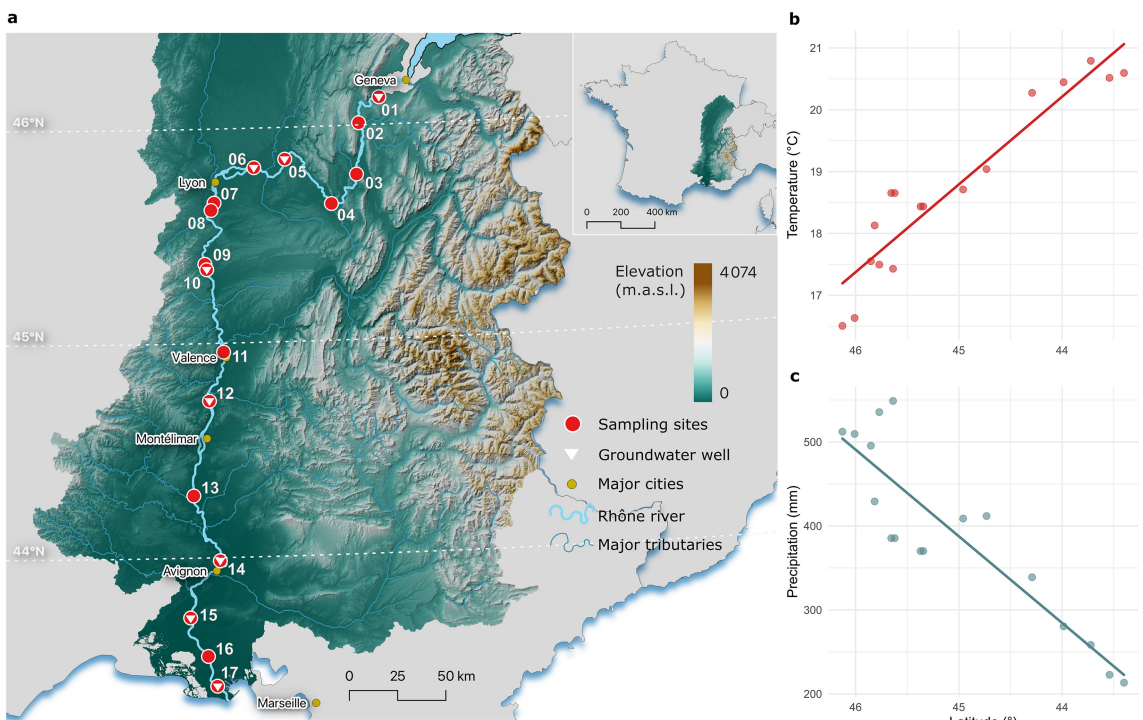


FIGURE 1 | (a) Location of sampling sites along the Rhône River corridor with major tributaries (SE France), (b) mean daily temperature and (c) mean cumulative precipitation during the growing season (April to September) from 1995 to 2022 for all sites as a function of their latitude.

Geographic Institute (IGN). We selected 17 forested sites along the Rhône River (France), which had been established for at least 30 years and had not undergone major cutting (Figure 1a). The forest at all sites was dense, with a closed-canopy, and the dominant trees were mainly *Fraxinus*, *Populus* and *Salix* species. Within each of these sites, we selected a square plot of at least 1 ha, specifically areas with dense, closed-canopy vegetation. These plots had similar species, maturity and stand density characteristics to maximise NDVI feedback on chlorophyll activity and their drivers. To ensure that these key criteria were met, we conducted a comprehensive visual analysis of all available ortho-photographs (<https://www.geoportail.gouv.fr>) for each potential site between 1980 and 2022. This careful examination allowed us to verify the age of the stands, assess their density, identify the primary tree species present and determine if any cuttings had occurred within the specified time frame. We divided these 17 sites into three groups of river section: upstream (Sites 1–6), midstream (Sites 7–12) and downstream (Sites 13–17).

2.3 | Data

2.3.1 | Remote Sensing

To measure NDVI over our sites, we used data from the Sentinel-2 (S2) satellite. S2 data provide multispectral information with a spatial resolution of 10–30 m and a temporal revisit of approximately four days (Li and Roy 2017). We acquired and preprocessed images using the Google Earth Engine (GEE) platform (<https://earthengine.google.com>). We selected Level 1C images (L1C, without atmospheric correction) from the S2 satellite instead of Level 2A (with atmospheric correction) because of the larger number of L1C images available on GEE between January 2016 and December 2022. Our focus was on the growing season, which we consider to be from April to September (Chmielewski and Rötzer 2001; Lobo-do Vale et al. 2019).

2.3.2 | Climate

We used gridded climate data derived from the E-OBS (<https://www.ecad.eu/>) gridded dataset based on satellite observations (Cornes et al. 2018). The E-OBS dataset provides a reasonable balance between spatial resolution (0.1°) and data accuracy (Bandhauer et al. 2022; Mavromatis and Voulanas 2021). We extracted the mean, maximum and minimum temperature and total precipitation data on a daily basis between 1995 and 2022.

2.3.3 | Groundwater Depth

Groundwater depth data play an important role in understanding water availability in riparian areas. To address this, we selected eight wells along the Rhône corridor near our study sites (Figure 1a) to estimate water availability in the phreatic zone that could benefit riparian phreatophyte tree species. The eight wells were located in the Rhône floodplain, within 1 km of the forest plots, to ensure an accurate representation of aquifer dynamics at our riparian sites. We retrieved the daily depth to groundwater (DTG) of these wells from the national database EauFrance via

HydroPortail from 2005 to 2022 (<https://www.hydro.eaufrance.fr/>). Although using only eight wells may not capture the full complexity of groundwater dynamics in the study area, particularly in regions with high human impact on groundwater levels, our choice of these wells provides a representative sample of the groundwater dynamics in the Rhône floodplain. These data were used to analyse how water availability in the phreatic zone affects NDVI and attenuates or accentuates climatic effects.

2.4 | Remote Sensing Data Processing

We performed several preprocessing steps on preselected L1C Sentinel images before calculating NDVI values. First, we filtered out all images with more than 20% cloud cover to limit the risk of bias, resulting in 2910 images for analysis, unevenly distributed over the study period (see Figure S1). We then applied an atmospheric correction using the Sensor Invariant Atmospheric Correction (SIAC) algorithm developed by Yin et al. (2019), which can correct for atmospheric effects on multiple sensors. This step provides a complete time series of bottom-of-atmosphere (BOA) images. In addition, we applied a cloud mask to exclude pixels covered by shadows or clouds, which could have affected the accuracy of our results. From this time series of preprocessed and corrected images, we derived NDVI using the near-infrared (NIR) and red (R) spectral bands using the following formula:

$$NDVI = \frac{NIR - R}{NIR + R}$$

The NDVI ranges from −1 to 1, with negative values representing nonvegetated surfaces, such as water, snow or bare soil, and positive values representing vegetated surfaces. NDVI values increase with chlorophyll activity (high chlorophyll content leads to increased absorption of red light and decreased reflectance, resulting in high NDVI values) and canopy density (Bannari et al. 1995; Huang et al. 2021). NDVI is also influenced by Leaf Area Index (the total area of leaves per unit of ground area) and soil background (Wang et al. 2005). From our sampling design, we expected NDVI to be mainly affected by differences in chlorophyll activity and plant stress to drought by selecting plots with continuous and dense canopies without any evidence of dieback due to disease or pest infestation. We further filtered the data by implementing a moving median filter (Cai et al. 2017) and a threshold of 0.2 to exclude any values not indicative of vegetation (Hashim, Abd Latif, and Adnan 2019; Taufik, Syed Ahmad, and Azmi 2019). Finally, we extracted monthly median NDVI values for each site (2016–2022) to analyse seasonal and interannual dynamics at the scale of the Rhône corridor.

Using these monthly NDVI time series, we calculated several phenological indices (Table S1) to analyse the intersite dynamics of the phenological cycle and to precisely define the different periods of the growing season. To extract phenological metrics from the NDVI time series, we used the phenofit package (Kong et al. 2022) in R, which defines phenological metrics from vegetation index time series extracted from Sentinel-2 satellites. The phenofit package allowed us to divide the growing season into several periods based on our monthly NDVI time series for

each site and year. To reconstruct a complete daily time series over the entire growing season, the phenofit package applies a weighted regression to create continuous time series by adjusting the weight of extreme values (see Figure S2). For our NDVI time series, we applied a weighted HANTS fitted regression, which performs best for vegetation with a clear and stable growing season (Bush et al. 2017; Yang et al. 2015). Based on this reconstructed NDVI time series, phenofit can be used to divide the growing season into different periods and to extract associated phenological metrics. To achieve this, the phenofit package determines the vegetative peak and two low periods. From this division, we extracted phenological metrics corresponding to the dates of the three main periods (see Figure S2). For this, we used the derivative method, which, according to Kong et al. (2022), is the most appropriate for our study because it provides three key phenological dates. Specifically, we extracted indices describing the onset, peak and end of the growing season, such as the start of the season (SOS), peak of the season (POS) and end of the season (EOS) (see Table S1).

To provide a clearer picture of the growing season, we divided it into three seasons based on the analysis of phenological variables extracted from the NDVI time series. On average, the early season started in late March, with a mean SOS at all sites on the 80th day of the year (DOY) (21 March). The NDVI then increased until it peaked in early June (mean POS = 152 DOY, around 1 June) (see Table S1). Since we mainly used monthly median NDVI, we rounded these dates to the nearest month. Thus, we considered the early season to begin in April and continue through May. For the midseason, we considered this season to begin in June. Because we have no metrics for the duration of the vegetative peak, we considered the entire month of June to be the midseason. Finally, the end of the growing season was defined by the EOS, which, on average, occurred in early October (mean EOS = 282 DOY, around October 9th). Therefore, we rounded the late season to the nearest month to avoid including values that were too low by the end of October. We defined the three seasons as April/May (early season), June (midseason) and July, August and September (late season) (de Jong et al. 2011).

2.5 | Hydrological and Climate Data Processing

To account for the lagged response of vegetation to climate variation, we calculated monthly mean temperature for each site from 2016 to 2022. To account for the effects of precipitation recharge before the months of the growing season, we incorporated a longer time lag by using 3-month cumulative precipitation. We evaluated different levels of precipitation accumulation and their correlations with NDVI through sensitivity analysis. Based on our results (see Table S2), we selected the total precipitation over the past 3 months.

To facilitate the comparison of groundwater data across sites, we calculated DTG anomalies by subtracting the average DTG value between 2005 and 2015 from each monthly value between 2016 and 2022. We used the average values between 2005 and 2015 at each site to establish a reference value over ten years, allowing us to compare DTG trends over the 2016–2022 period. We used these 10 years because we were unable to obtain older

data for all wells. Nevertheless, we consider these 10 years to be fairly representative of the hydrological situation, given the relative hydrological stability of the Rhône as a result of the numerous hydraulic schemes that regulate its flow (Bravard and Gaydou 2015). Finally, to consider the lagged response of vegetation to variations in groundwater depth, we calculated the mean DTG anomalies over the previous 2 months.

2.6 | Analysis of NDVI Variability and Relationships With Hydroclimatic Variables

The main objectives of this first part of the analysis were (1) to analyse temporal variations in NDVI, whether inter- or intra-annual, in relation to the latitudinal gradient and (2) to quantify the role of hydroclimatic variables on NDVI at different temporal and spatial scales. All data analyses and statistical tests were performed using the R programming language, version 4.3.0 (Team 2022).

First, we quantified and compared the linear relationships between monthly median NDVI and latitude to investigate the effect of latitude on NDVI during the growing season. We then analysed the interannual variability of NDVI and tested the difference in means between years using one-way ANOVAs for each river section (upstream, midstream and downstream). Finally, posthoc pairwise comparisons were computed using Tukey's Honest Significant Difference at the 95% confidence level.

Second, to visualise the spatiotemporal variability of the effects of hydroclimatic variables on monthly NDVI, we computed Pearson correlation coefficients between the monthly median NDVI values obtained at each site between April and September and two climate variables. We used total precipitation accumulated over the last 3 months and daily mean temperature averaged by river section (upstream, midstream and downstream sites) and season (early, mid and late). For the groundwater depth data, we analysed available data from the eight sites (Figure 1a). Similar to the analysis of climate variables, we calculated the Pearson correlation coefficient between NDVI and groundwater depth data for each of the eight sites.

Finally, to examine the relationship between climate variables and NDVI by season and river section, we used monthly median NDVI values at each site for each year from 2016 to 2022. The monthly NDVI medians were compared to the average accumulated precipitation over the last 3 months. We followed the same methodology for temperature, but did not account for a 3-month lag and used monthly mean temperature. We conducted linear regressions and evaluated the significance of each regression to examine the correlations between climate variables and NDVI.

2.7 | Climate Mixed-Effects Model for NDVI Prediction

To determine the influence of climate variables on NDVI variation and the role of latitude, we compared different linear mixed-effects models (using the lme4 package), including both the site effect and year as random variables to account for influences on greenness unattributable to climate factors alone. We first built

two reference models: a null model with no fixed effect ($\text{NDVI} \sim 1 + (\text{1|Year}) + (\text{1|Site})$) and a latitude-only model with latitude as the only fixed effect ($\text{NDVI} \sim \text{Latitude} + (\text{1|Year}) + (\text{1|Site})$). The latitude-only model was included as a reference as an alternative to models that included temperature and/or precipitation as explanatory variables. We ran these two reference models for each of the three seasons (early, mid and late), resulting in six models. These reference models served as a basis for assessing the role of climate variables on NDVI relative to latitude as a simple geographic proxy variable. We then developed several climate models for each season. In these climate models, we used the two main climate variables: mean monthly temperature and total precipitation over the last 3 months. Four separate models were created: temperature only, precipitation only, temperature and precipitation without interaction and temperature and precipitation with interaction. Together with the reference models, we evaluated 18 models (six types of models for each of the three seasons).

Akaike's Information Criteria (AIC) was used to evaluate and compare the performance of each model (Burnham and Anderson 2004; Mazerolle 2020). In all cases, model residuals were visually assessed to verify linear model assumptions (Osborne and Waters 2019). To compare the influence of variables in predicting NDVI, we evaluated the sign and significance of each coefficient estimate of the best model for each season. To allow comparisons between different climate variables, we standardised and centred the data.

Finally, we wanted to see if DTG anomalies had a significant influence on NDVI. For this, we developed three additional mixed-effects models with the same random factors (site and year) but with only the 2-month DTG anomalies as a fixed factor and only at the eight sites with DTG data. We evaluated the sign and significance of the coefficient estimates of each model to assess the effect of groundwater level variations on NDVI at the eight sites in the three different periods of the growing season.

3 | Results

3.1 | Spatio-Temporal Variability of NDVI and Phenology

Analysis of the annual median NDVI data over the study area (Figure 2a) showed a significant positive trend in NDVI with latitude ($R^2 = 0.75$; $p < 0.001$). Monthly trends in NDVI during the growing season showed an inversion of the north-south gradient as the seasonal phenology progressed from March to September (Figure 2b). The linear relationship between NDVI and latitude is significant for every month ($p < 0.05$), with March being nearly significant ($p = 0.056$) (see Table S3). In June and July, NDVI was most closely related to latitude ($R^2 = 0.85$), but this relationship was weaker in the early and late season months. In March (before the onset of the growing season), NDVI increased at lower latitudes, which is consistent with the trend observed in April, suggesting an earlier onset of green-up in the southern region, with a relatively high NDVI in April. Vegetative greenness peaked in May at higher latitudes and in June at lower latitudes. The trend then reversed, with vegetative greenness decreasing at lower latitudes and reaching a minimum in September. Finally, there was a generalised drop in greenness from June onwards, with an overall decrease in NDVI at all sites. To facilitate the interpretation of monthly NDVI trends (Figure 2b), we provide an animation of the monthly evolution of the NDVI gradient in the S.I. (Fig. S3).

Phenology analysis revealed differences in the timing of the growing season along the Rhône River, especially at the onset of the growing season. These differences were expressed at different temporal and spatial scales. Indeed, an interannual variation of the SOS was observed, with a time lag of up to 15 days between two different years (Figure 3a). Spatial variability along the hydroclimatic gradient also revealed intersite temporal variability (Figure 3b). On average, downstream riparian sites had a mean onset on the 69th day of the year (March 10), while upstream sites

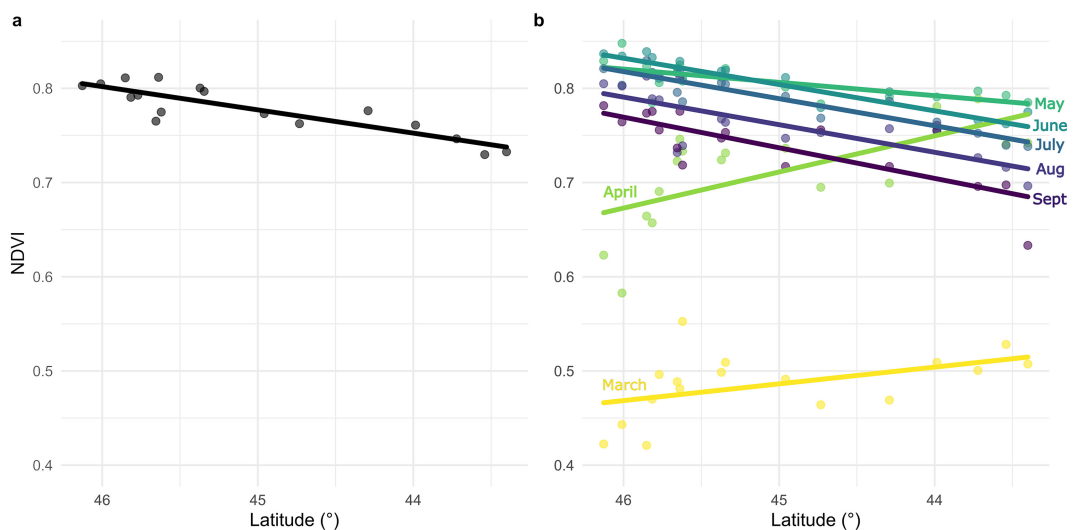


FIGURE 2 | (a) Annual median NDVI over the growing season (April–September) and (b) seasonal variability of the monthly median NDVI between March and September (2016–2022) across all 17 sites, ranked by latitude. Latitude on the x-axis is inverted to match the hydroclimatic gradient from north to south. The colour gradient is used for readability only.

had a mean onset on the 91st day (April 1), a lag of 22 days. The linear relationship between median SOS and latitude was significant ($R^2 = 0.80$; $p < 0.001$), indicating that there is a lag of 9.77 days for one degree of latitude (see Figure S4). The other two phenological metrics showed different responses than SOS. In fact, POS (Figure 3c) was not reached earlier in the south, despite what the earlier onset of SOS would suggest. There was considerable intersite and intrasite variability and no significant relationship between POS and latitude ($p = 0.53$; see Figure S4). In contrast, EOS showed an inverse pattern to the SOS in its response to the latitudinal gradient, with EOS occurring earlier in the north than in the south (Figure 3d). This is true up to site 15, which has the latest EOS date of all sites. However, this date decreased at the two southernmost sites (S16 and S17). Despite this decreasing trend at the southernmost sites, there was a strong and significant correlation between EOS and latitude ($R^2 = 0.66$; $p < 0.001$; see Figure S4).

Interannual analysis of the NDVI between 2016 and 2022 in each river section showed significant differences (Figure 4). For example, at the upstream sites, according to the post-hoc test, 2021 stood out significantly from the other years, with a much lower NDVI. This difference for 2021 was also found in the midstream group, but the post-hoc test indicated that the average NDVI in 2021 remained similar to that of 2018, 2019, 2020 and 2022. For downstream, the average NDVI in 2021 was not significantly different from the other years. On the contrary, the average NDVI for 2022 was similar to the other years for upstream and midstream, whereas it was different from the other years for downstream, indicating a lower average NDVI than

for the rest of the period. This observation can also be made for 2016, where NDVI was significantly different from other years on midstream and to a lesser extent on downstream, but not on upstream.

3.2 | Hydroclimatic Controls on Spatiotemporal Variability of NDVI

Pearson's correlation analysis (Table 1) showed that monthly median NDVI was significantly correlated with monthly mean temperature across all groups of sites and seasons. However, the correlation trends differed between groups and seasons. Specifically, we found a positive correlation between NDVI and temperature during the early and late seasons, with stronger correlations observed in the upstream group ($r = 0.578$ and $r = 0.518$) than in the midstream ($r = 0.414$ and $r = 0.327$) and downstream ($r = 0.316$ and $r = 0.279$) groups. In contrast, a negative correlation was observed between NDVI and temperature during the midseason, with stronger correlations and lower p -values observed in the downstream group ($r = -0.616$; $p < 0.001$) compared to the upstream group ($r = -0.451$; $p = 0.003$). With precipitation, we observed a positive correlation between NDVI and 3-month precipitation during the mid and late seasons in the downstream group. A positive correlation was also observed during the early and late seasons in the midstream group. In contrast, no significant correlation was found in the upstream group. Finally, we found no significant correlation between NDVI and groundwater anomalies, except for a positive correlation during the late season in the downstream group

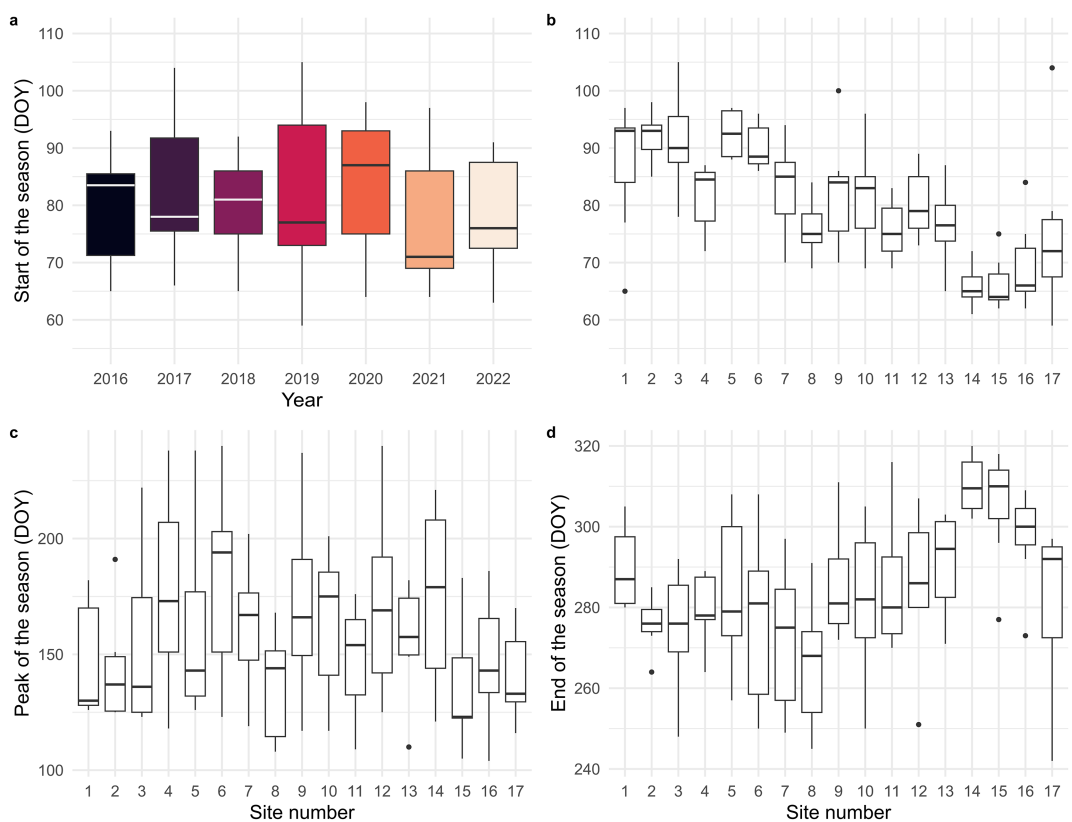


FIGURE 3 | (a) Annual box plots showing the start of the season (SOS) for each year between 2016 and 2022; colours refer to years only. Box plots by site over each year showing: (b) the start of the season, (c) the peak of the season and (d) the end of the season. Sites are numbered from upstream to downstream.

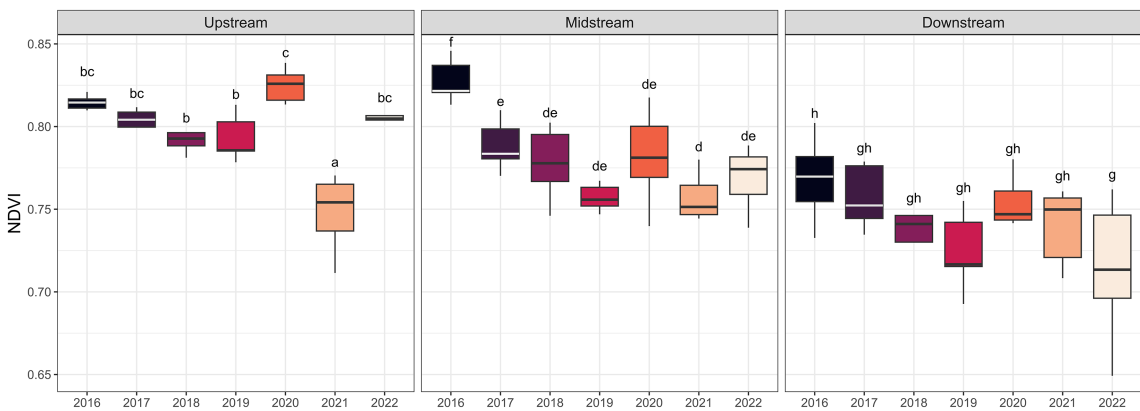


FIGURE 4 | Interannual variation of NDVI between 2016 and 2022 on growing season months divided by groups of sites. Boxplot not sharing letters differed significantly within a site group at the 95% confidence level ($p < 0.05$) in Tukey's honest significant difference post hoc tests.

TABLE 1 | Pearson correlations between monthly NDVI and hydroclimate variables divided by spatio-temporal attributes (season and latitude) on growing season months from 2016 to 2022.

		Upstream		Midstream		Downstream	
Hydroclimate variable		<i>r</i>	<i>p</i>	<i>r</i>	<i>p</i>	<i>r</i>	<i>p</i>
Early	Mean temperature	0.578	<0.001	0.414	<0.001	0.316	0.010
	3-month precipitation	0.183	0.114	0.390	<0.001	0.048	0.706
	Groundwater ^a	-0.032	0.853	0.148	0.470	0.264	0.104
Mid	Mean temperature	-0.451	0.003	-0.646	<0.001	-0.616	<0.001
	3-month precipitation	0.193	0.222	0.129	0.417	0.445	0.007
	Groundwater ^a	-0.291	0.214	0.526	0.053	0.068	0.770
Late	Mean temperature	0.518	<0.001	0.327	<0.001	0.279	0.004
	3-month precipitation	0.046	0.616	0.300	<0.001	0.380	<0.001
	Groundwater ^a	-0.077	0.559	0.185	0.253	0.321	0.011

Note: **Bold text** indicates significant correlations at $p < 0.05$, coloured cells indicate where the *R* is significant; they are green for positive correlation and red for negative correlation. The early season consists of April and May, the midseason of June and the late season of July, August and September. The upstream group is composed of sites 1 to 6, midstream of sites 7 to 12 and downstream of sites 13 to 17.

^aOnly eight sites.

($r = 0.321$; $p = 0.011$) and a nearly significant positive correlation during the midseason in the midstream group ($r = 0.526$; $p = 0.053$).

Analysis of the relationship between monthly NDVI and monthly mean temperature revealed two distinct trends (Figure 5a). First, in the early season, NDVI was significantly influenced by temperature, with higher NDVI as temperature increased. Temperature was a good predictor of NDVI, especially at upstream sites where the linear relationship had a higher R^2 ($R^2 = 0.33$, $p < 0.001$) than at midstream and downstream sites ($R^2 = 0.17$ and $p < 0.001$, $R^2 = 0.10$ and $p = 0.01$, respectively). The situation is similar for the late season, where R^2 values are higher at upstream sites ($R^2 = 0.27$, $p < 0.001$) than at midstream and downstream sites ($R^2 = 0.11$ and $p < 0.001$, $R^2 = 0.08$ and $p = 0.003$, respectively), indicating a greater positive effect of temperature on NDVI at higher latitudes. In contrast, temperature

had a negative effect on NDVI in the midseason. This time, the effect of temperature on NDVI was more pronounced at midstream and downstream sites ($R^2 = 0.42$ and $p < 0.001$, $R^2 = 0.38$ and $p < 0.001$, respectively) than at upstream sites ($R^2 = 0.20$, $p = 0.003$). Linear regressions between precipitation and NDVI showed more spatial heterogeneity compared to temperature (Figure 5b). In fact, there were no significant linear regressions at any growing season period at upstream sites ($p > 0.05$). At midstream and downstream sites, we observed a positive and significant relationship between precipitation and NDVI in the late season ($R^2 = 0.10$ and $p < 0.001$, $R^2 = 0.14$ and $p < 0.001$, respectively). In the early season and midseason, there were contrasting relationships between precipitation and NDVI at both groups of sites. In the early season, the relationship was positively significant in midstream sites but not at downstream sites, while the opposite was true for the midseason. These relationships, even when significant, had low R^2 .

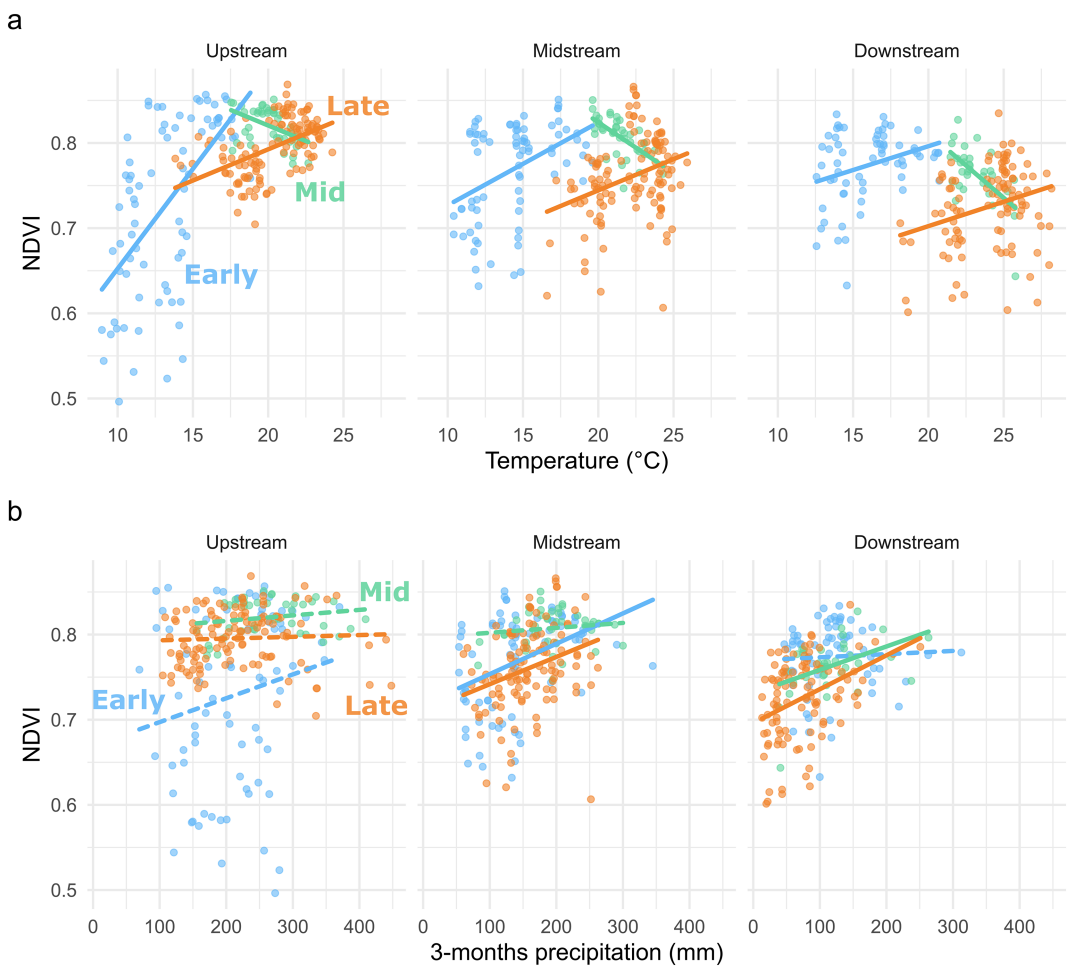


FIGURE 5 | Monthly median NDVI values for each growing season period and river section with (a) mean temperature and (b) 3-month accumulated precipitation over the same period. Each dot represents a monthly value per site. Solid lines indicate a significant relationship ($p < 0.05$).

3.3 | NDVI Prediction From Climate Model

Model ranking (Table 2) showed that the model with both climate variables considering their interaction ($\text{NDVI} \sim \text{Temperature} + 3\text{-months precipitation} + \text{Temperature} * 3\text{-months precipitation} + (1| \text{Year}) + (1| \text{Site})$) was the best fitting model for each season. However, this observation was particularly true for the early season, where the climate model with interaction ($\text{Temp_Precip_interaction_early}$) carried 99.8% of the AIC weight. The second model (Temperature_early) carried only 0.1% of the AIC weight ($\Delta \text{AIC} = 13.58$), indicating the strength of the full interaction model in predicting NDVI compared to all other models. The two reference models (Latitude_early and Null_early) had among the highest ΔAIC ($\Delta \text{AIC} = 99.05$ and $\Delta \text{AIC} = 103.25$, respectively), indicating that they poorly explained NDVI in the early season.

For predicting midseason NDVI, the temperature/precipitation-interaction model was also the best model but less dominant than for the early season model, carrying only 62% of the AIC weight, while the second best model, with Latitude as the single fixed factor, had ΔAIC of 1.11 and an AIC weight of 35.6%. The climate model without interaction (Temp_Precip_mid) and the temperature-only model (Temperature_mid) had substantially higher ΔAIC (7.72 and 8.23, respectively) and

comprised only about 1% of the AIC weight for each. The pattern was similar for the late season, with two models sharing 64.5% and 35.5% of the AIC weight. However, this time, the second model was the temperature/precipitation model without interaction (Temp_Precip_late), with a ΔAIC of less than 2 ($\Delta \text{AIC} = 1.19$). No other models had any appreciable explanatory power, and the two reference models had the highest ΔAIC across the candidate model set ($\Delta \text{AIC} = 71.79$ for the Latitude_late model and $\Delta \text{AIC} = 90.71$ for the Null_late model).

The analysis of the effect of the climate variables of the best-fitting models for each growing season period, i.e., the climate model with interaction ($\text{Temp_Precip_interaction}$) in each case, showed different trends depending on the season (Figure 6). A positive coefficient estimate indicates that an increase in a variable leads to an increase in NDVI. In the early season, an increase in temperature led to an increase in NDVI, independently of other climate variables, year and latitude. The same trend was observed in the late season but was reversed in the midseason, with NDVI decreasing as temperature increased. In each season, the effect of temperature on NDVI was highly significant ($p < 0.001$). Total precipitation over the last 3 months had an overall positive effect on NDVI but was relatively insignificant, except in the late season. In contrast, the interaction between

TABLE 2 | Model rankings by season (early, mid and late) for the linear mixed-effects regression models with NDVI as the dependent variable and site and year as random effects.

AIC comparison					
Model	K	AIC	Delta AIC	AIC weight	Cum weight
Early					
Temp_Precip_interaction_early	7.000	-613.930	0.000	0.998	0.998
Temperature_early	5.000	-600.350	13.581	0.001	0.999
Temp_Precip_early	6.000	-600.016	13.915	0.001	1.000
Latitude_early	5.000	-514.883	99.047	0.000	1.000
Null_early	4.000	-510.685	103.246	0.000	1.000
Precipitation_early	5.000	-510.336	103.595	0.000	1.000
Mid					
Temp_Precip_interaction_mid	7.000	-584.754	0.000	0.620	0.620
Latitude_mid	5.000	-583.646	1.108	0.356	0.977
Temp_Precip_mid	6.000	-577.030	7.724	0.013	0.990
Temperature_mid	5.000	-576.528	8.227	0.010	1.000
Null_mid	4.000	-547.858	36.896	0.000	1.000
Precipitation_mid	5.000	-545.842	38.912	0.000	1.000
Late					
Temp_Precip_interaction_late	7.000	-1311.169	0.000	0.645	0.645
Temp_Precip_late	6.000	-1309.979	1.190	0.355	1.000
Temperature_late	5.000	-1290.718	20.451	0.000	1.000
Precipitation_late	5.000	-1253.781	57.388	0.000	1.000
Latitude_late	5.000	-1239.378	71.790	0.000	1.000
Null_late	4.000	-1220.455	90.714	0.000	1.000

temperature and precipitation had a significant effect on NDVI in the early season and midseason but not in the late season. This means that the two main effects, temperature and precipitation, were stronger predictors than including the interaction term, indicating that temperature/precipitation were not dependent on the values of precipitation/temperature.

Estimates of the mixed-effect models with 2-month DTG anomalies showed that overall DTG positively influenced NDVI throughout the growing season (Figure 7). Positive DTG anomalies resulted in higher NDVI values independent of year and latitude. Results from seasonal models showed that DTG anomalies had no significant effect on NDVI in the early season and midseason. However, a positive and significant effect of DTG anomalies on NDVI was observed in the late season.

4 | Discussion

Our study investigates riparian tree greenness as determined by NDVI and provides insights into the intricate relationship between hydroclimatic factors and riparian tree health. Focusing on a 500-km-long north-south river corridor, our research sheds light

on the variability of riparian greenness and the various climate controls that influence it, facilitating the design of landscape-scale riparian ecosystem restoration strategies tailored to the specific local climatic context. Our results showed that riparian greenness within a large river corridor is mainly regulated by climate control, which exhibits spatial and temporal variability throughout the growing season. Notably, there was an overall transition in climate control, with temperature initially controlling greenness and precipitation increasingly factoring into the equation during the summer (Tables 1 and 2). These climate controls regulate the balance between evapotranspiration and precipitation, thus determining evaporative water demand and soil moisture at varying timescales along the latitudinal gradient. During drought periods, sites with high groundwater availability showed greater resilience to climate controls by using different water sources, allowing them to maintain high levels of greenness (Figure 7).

4.1 | Riparian Tree Greenness: From Temperature-Limited to Water-Limited

The effect of the hydroclimatic gradient on riparian greenness leads to high variability in NDVI. This variability occurs

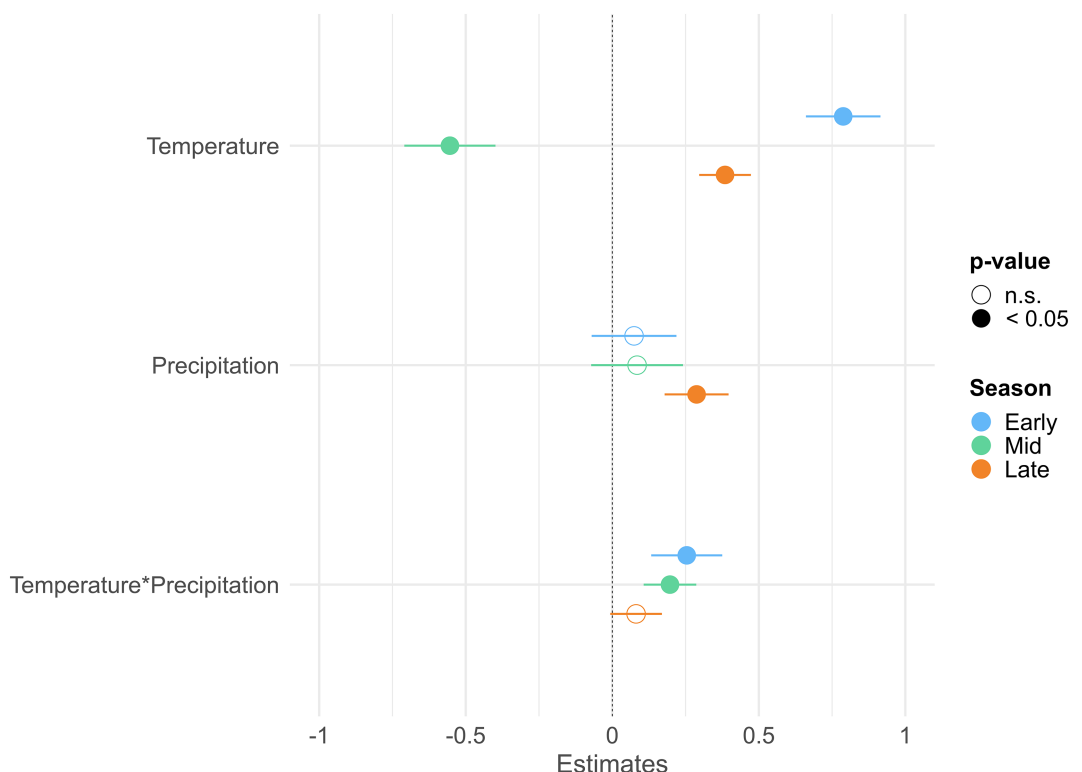


FIGURE 6 | Estimates of the two climate variables and their interaction from climate-interaction models for each season. A filled dot indicates that the effect of the variable on NDVI is statistically significant ($p < 0.05$).

seasonally, with an earlier onset of the growing season at downstream sites (Figure 3b) or interannually with high variability between years and river sections (Figure 4). This high variability of NDVI can be attributed to the latitudinal gradient of the Rhône River corridor, which is expressed through climate variability, such as temperature and precipitation, which are functions of latitude (Figure 1b,c). As latitude decreases, temperature increases and precipitation decreases in a near-linear manner. Our findings suggest that the greenness of riparian trees during the growing season is closely tied to latitude, with lower NDVI values as the latitude decreases (see Figure 2a). This correlation aligns with previous research demonstrating the significance of temperature and precipitation in regulating the greenness of riparian trees (Fu and Burgher 2015; Pace et al. 2021). However, our findings demonstrate that NDVI or phenological metrics reveal nonlinear responses to latitude/climate fluctuations (Figures 3 and 4). These nonlinear responses convey significant spatial and temporal disparities in climate controls on greenness, suggesting that the latitude/climate gradient is not the only factor influencing NDVI. The analysis of the relationships between NDVI and hydroclimate variables (Table 1) demonstrates that climate controls are spatially and temporally heterogeneous, depending on the river section and growing season periods. This variability of climate controls on greenness has also been shown along an altitudinal gradient in different vegetation types (Piedallu et al. 2019).

Temperature plays a critical role in determining the greenness of riparian trees. According to mixed-effects models, temperature is a strong predictor of NDVI (Table 2), with varying effects during the growing season (Figure 6). Phenological onset

is primarily controlled by temperature (Chen et al. 2019; Fu et al. 2014; Menzel et al. 2006). Our findings confirm this trend, with downstream sites (Figure 3b) having an earlier start of the growing season due to warmer conditions earlier in the season. However, at the vegetative peak (midseason), temperature has a negative influence on greenness. This limiting aspect of temperature is found under several conditions (Liu et al. 2015; Piedallu et al. 2019; Warter et al. 2023) but appears to be more prevalent in semi-arid environments (Fu and Burgher 2015; Yao et al. 2018). Our findings are consistent with these observations, as we found a more pronounced effect of temperature in downstream and midstream sites than in upstream sites (Table 1). Finally, the role of temperature is even more heterogeneous in the late season. During this period, NDVI is positively influenced by temperature (Figure 6). However, Figure 5 and Table 1 show that the effect of temperature is highly variable along the hydroclimatic gradient. Upstream, temperature has a significant positive effect on NDVI, while downstream this effect decreases and becomes less significant (Table 1). High temperatures in semi-arid environments, such as downstream, can negatively affect photosynthetic activity and accelerate senescence (Adams et al. 2015; Hew, Krotkov, and Canvin 1969), whereas in temperate climates they tend to extend the growing season and delay senescence (Chen et al. 2019; Fu et al. 2018; Vitasse et al. 2009).

Precipitation tends to have a more limited temporal and spatial effect on NDVI variability (Table 2). At the onset and peak of the growing season, greenness does not appear to be directly influenced by precipitation (Figure 6). This observation that greenness is not limited by the lack of early season and midseason precipitation

makes sense, given that riparian trees along the Rhône benefit from good vadose zone recharge from winter precipitation and high streamflow from snowmelt runoff, which maintains relatively high groundwater levels (Sargeant and Singer 2021). This limited effect of precipitation on greenness has been highlighted in several environments (Piedallu et al. 2019); however other studies have shown the opposite effect, especially in semi-arid climates (Chen et al. 2014; Grossiord et al. 2017; Vicente-Serrano et al. 2013), more similar to that observed for the late season. Indeed, the situation is different for the late season, with the precipitation model being more highly ranked (Table 2) and having a notably positive effect on the level of greenness (Figure 6). This suggests that recharge by precipitation over the last 3 months plays a major role in maintaining greenness during the driest periods and at locations where the evapotranspiration/precipitation balance is significantly affected by rising temperatures. In temperate climates, other studies indicate that cumulative precipitation over longer periods can also have a significant impact on the greenness of riparian trees (Pace et al. 2021).

Our results also highlight the importance of considering the interactions between precipitation and temperature. Indeed, these two climate factors are the two most important contributors to the water balance, which is itself strongly linked to tree growth (Bréda et al. 2006). However, our results show that, in every season, the model that considers the interaction between these two climate variables ranks higher than that without interaction (Table 2). These results confirm the importance of considering this interaction in NDVI prediction models, as the combined effect of these two climatic controls will strongly affect the water balance and thus the growth of riparian trees.

However, explaining NDVI variations by precipitation and temperature alone does not explain all the variance in NDVI (Piedallu et al. 2019). This is particularly true in semi-arid environments subject to high water stress, where the role of local water availability seems to have a predominant impact on riparian tree growth (Sabathier et al. 2021; Schook et al. 2020; Singer et al. 2013).

4.2 | Local Water Availability: A Key to Improve Riparian Forest Resilience?

Although climate variations seem to explain an important part of the variability in NDVI, local water availability conditions can attenuate or accentuate climate effects. Our results for the eight study sites with groundwater depth data show that when groundwater anomalies are positive, NDVI benefits (Figure 7). This observation is significant for the growing season as a whole, but when broken down into three periods, we observe a real and significant positive impact of the DTG anomalies on the late season only. This result is in line with our observations on climate variables at all sites, where we note that the late season is the most dependent period on water recharge by precipitation. During this period, which is the hottest and driest of the growing season, the evapotranspiration/precipitation balance is often impacted by the lack of precipitation, especially in downstream sites. Increased evaporative demand puts further pressure on soil moisture, reducing water availability in the vadose zone. To withstand drought, riparian trees, most of which are phreatophytes, depend on access to water in the phreatic zone (Dufour and Piégay 2008; Singer et al. 2013). When climate controls strongly affect the evapotranspiration/precipitation

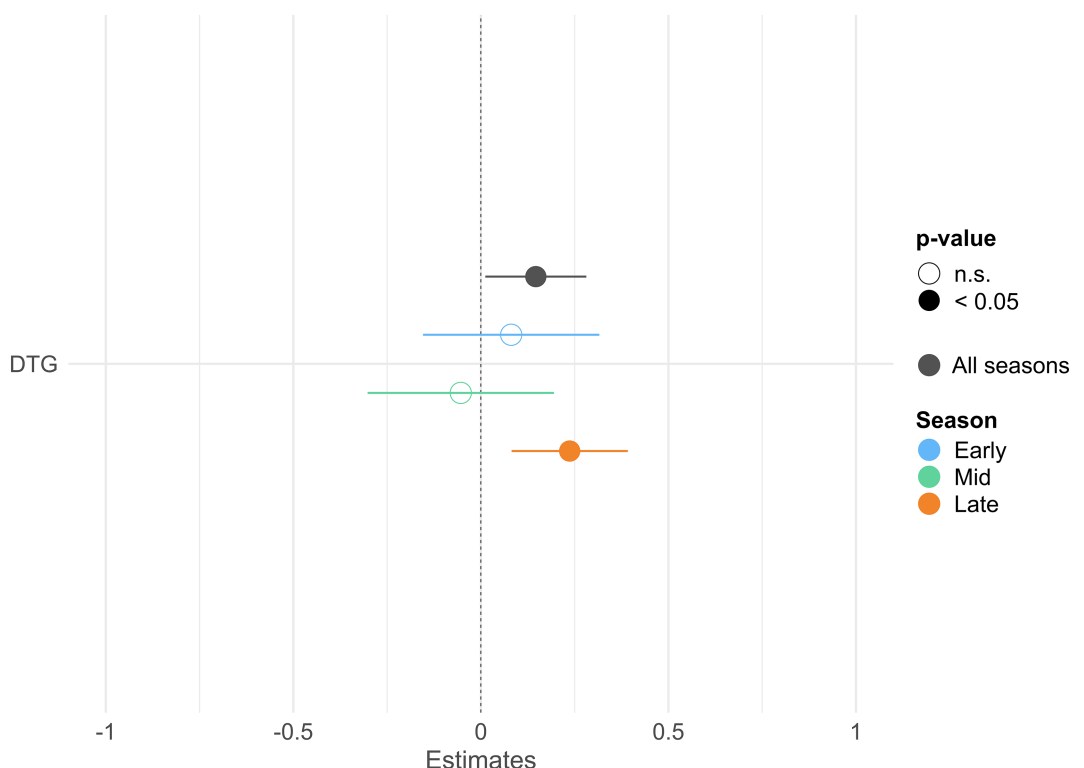


FIGURE 7 | Estimates of depth to groundwater variable from linear mixed-effect models of each season with DTG as a fixed factor and latitude and year as random factor. A filled dot indicates that the effect of the variable on NDVI is statistically significant ($p < 0.05$).

balance, sites with good water availability in the phreatic zone will be more resistant.

In our study, we were unable to obtain groundwater data for all sites, just as we were unable to characterise other geomorphological parameters that could influence water availability, such as the thickness of fine sediment. However, geomorphological parameters can strongly influence water availability conditions and therefore influence the resilience of riparian trees to drought episodes. A site benefiting from geomorphological conditions favouring good water availability, such as a thick layer of fine sediment allowing significant storage in the vadose zone that is valuable for hardwood species such as *Fraxinus* (Singer et al. 2014) or the presence of a shallow water table that is valuable for phreatophytes, results in higher greenness (Figure 7). In addition to geomorphological conditions, other factors can positively or negatively influence NDVI, such as species richness (Wang et al. 2016), genetic diversity (Evans et al. 2016) and species distribution (Lloret et al. 2007). Some studies have also shown the importance of soil-related effects on NDVI (Bergès and Balandier 2010; Walker et al. 2003). NDVI can also be influenced by reach-specific conditions. For example, along the Rhône, water levels in diverted channels are frequently very low, drastically reducing water availability for riparian stands (Fruget and Dessaix 2003). Similarly, high levels of groundwater extraction can drastically reduce water availability in the phreatic zone and therefore have a significant impact on NDVI (Rohde et al. 2021). As with other geomorphological factors, accounting for these factors is difficult, as it requires accurate and homogeneous data at the fluvial corridor scale. These factors may improve the prediction of our model, but our results are consistent with other studies that have attempted to explain the spatiotemporal variability of NDVI using climatic variables (Pace et al. 2021).

4.3 | Insight Into Future Trends and Management Solutions

Our retrospective analysis of the impact of climate controls on greenness revealed a high degree of variability depending on the year, season and local climatic context. As a result, it seems difficult to predict exactly where and to what extent climate controls will affect greenness along a river corridor characterised by a hydroclimatic gradient. However, our study provides a better characterisation of the relationships between climate controls and greenness along a large river. Indeed, of all the climate controls evaluated in our study, temperature is the one with the largest effect. However, rising temperatures related to climate change will accentuate the effect of temperature on greenness. This increase in temperature along the hydroclimatic gradient will affect all riparian stands in the river corridor through both local and nonlocal climate controls. During the warmest period of the growing season, water availability in the root zone can decline rapidly due to indirect temperature-related controls on water availability, such as increased evapotranspiration (Serrat-Capdevila et al. 2011; Zhang et al. 2015). Increased atmospheric demand can rapidly shift the balance between evapotranspiration and precipitation that regulates soil moisture. These shifts occur more rapidly at sites further south along the hydroclimatic gradient, where precipitation is lower and evapotranspiration is higher. These new forcings can

shift the evapotranspiration/precipitation balance and significantly increase water stress in riparian stands that were previously unaffected by water stress. Situations of greenness limitation observed in downstream sites will more regularly affect midstream and even upstream sites. These changes could lead to an increase in the physiological and morphological responses of trees. As these responses become more pronounced, they could lead to canopy dieback and tree mortality, as shown in highly disconnected conditions following channel incision (Stella et al. 2013) and then to profound changes in forest composition, ecosystem services and carbon sequestration (Bréda et al. 2006; Sarris, Christodoulakis, and Körner 2011; Tai et al. 2018). These pressures on riparian ecosystems highlight the importance of identifying not only the climate controls on vegetative greenness but also the local controls that can significantly influence the resilience of riparian stands.

In the face of these global climate changes, our NDVI climate model is proving to be an interesting tool for assessing the sensitivity of forest patches to climate change and their potential resilience according to their degree of dependence on climatic conditions. We could continue this work by using projected climate change scenarios to visualise the effects of rising temperatures on the climatic control of water availability and, therefore, on the greenness of riparian trees. This work provides a better understanding of the spatial variation in climate controls on greenness, allowing better adaptation of management measures to promote greater resilience of riparian forests, such as increasing minimum flows in bypassed reaches or reducing groundwater pumping.

5 | Conclusion

In this study, we analysed the relationships between hydroclimatic variables and riparian greenness along the hydroclimatic gradient of the Rhône River. We found that the impact of climatic variables on greenness varied according to spatial and temporal variations. Temperature was the primary limiting factor in northern areas, while water availability was the main limitation in southern areas. These hydroclimatic variations have different effects on greenness. We show that areas affected by reduced water availability have lower greenness as trees develop mechanisms to mitigate water stress. A better understanding of these climatic controls on the vegetative dynamics of riparian forests is a major challenge in the face of rising temperatures and decreasing water availability. Areas facing little or no constraint will experience new water availability issues, while areas already constrained by water availability will experience species survival issues. In general, the vulnerability of riparian forests is increasing; therefore, it is necessary to implement measures to restore or protect riparian forests in accordance with the local context, taking into account spatiotemporal hydroclimatic variations.

Author Contributions

Pierre Lochin: conceptualisation, data curation, methodology, formal analysis, writing – original draft, writing – review and editing. **Hervé Piégay:** conceptualisation, methodology, funding acquisition, supervision, writing – review and editing. **John C. Stella:** conceptualisation, methodology, funding acquisition, supervision, writing – review and editing. **Kelly K. Taylor:** methodology, writing

– review and editing. **Lise Vaudor:** methodology, data curation, writing – review and editing. **Michael Bliss Singer:** conceptualisation, methodology, funding acquisition, supervision, writing – review and editing.

Acknowledgements

This work was supported by the Graduate School H2O'Lyon (ANR-17-EURE-0018) of Université de Lyon (UdL), within the program “Investissements d’Avenir” operated by the French National Research Agency (ANR), by the National Science Foundation (EAR 1700517, EAR 1700555 and BCS 1660490) and by the US Department of Defense’s Strategic Environmental Research and Development Program-SERDP (RC18-1006).

Data Availability Statement

Data sources for this study are publicly available, and data used for analyses are available from the authors upon request.

References

- Adams, H. D., A. D. Collins, S. P. Briggs, et al. 2015. “Experimental Drought and Heat Can Delay Phenological Development and Reduce Foliar and Shoot Growth in Semiarid Trees.” *Global Change Biology* 21, no. 11: 4210–4220. <https://onlinelibrary.wiley.com/doi/abs/10.1111/gcb.13030>.
- Allen, D. D. Breshears, and N. G. McDowell. 2015. “On Underestimation of Global Vulnerability to Tree Mortality and Forest Die-Off From Hotter Drought in the Anthropocene.” *Ecosphere* 6, no. 8: art129. <https://onlinelibrary.wiley.com/doi/abs/10.1890/ES15-00203.1>.
- Bandhauer, M., F. Isotta, M. Lakatos, et al. 2022. “Evaluation of Daily Precipitation Analyses in E-OBS (v19.0e) and ERA5 by Comparison to Regional High-Resolution Datasets in European Regions.” *International Journal of Climatology* 42, no. 2: 727–747. <https://onlinelibrary.wiley.com/doi/abs/10.1002/joc.7269>.
- Bannari, A., D. Morin, F. Bonn, and A. R. Huete. 1995. “A Review of Vegetation Indices.” *Remote Sensing Reviews* 13, no. 1–2: 95–120. <https://doi.org/10.1080/02757259509532298>.
- Berg, A., and J. Sheffield. 2018. “Climate Change and Drought: The Soil Moisture Perspective.” *Current Climate Change Reports* 4, no. 2: 180–191. <https://doi.org/10.1007/s40641-018-0095-0>.
- Bergès, L., and P. Balandier. 2010. “Revisiting the Use of Soil Water Budget Assessment to Predict Site Productivity of Sessile Oak (*Quercus petraea* Liebl.) in the Perspective of Climate Change.” *European Journal of Forest Research* 129, no. 2: 199–208. <https://doi.org/10.1007/s10342-009-0315-1>.
- Bravard, J. P., and P. Gaydou. 2015. “Historical Development and Integrated Management of the Rhône River Floodplain, From the Alps to the Camargue Delta, France.” In *Geomorphic Approaches to Integrated Floodplain Management of Lowland Fluvial Systems in North America and Europe*, 289–320. Springer. https://doi.org/10.1007/978-1-4939-2380-9_12.
- Bréda, N., R. Huc, A. Granier, and E. Dreyer. 2006. “Temperate Forest Trees and Stands Under Severe Drought: A Review of Ecophysiological Responses, Adaptation Processes and Long-Term Consequences.” *Annals of Forest Science* 63, no. 6: 625–644. <https://doi.org/10.1051/forest:2006042>.
- K. P. Burnham, and D. R. Anderson, eds. 2004. *Model Selection and Multimodel Inference*. New York, NY: Springer. <http://link.springer.com/10.1007/b97636>.
- Bush, E. R., K. A. Abernethy, K. Jeffery, et al. 2017. “Fourier Analysis to Detect Phenological Cycles Using Long-Term Tropical Field Data and Simulations.” *Methods in Ecology and Evolution* 8, no. 5: 530–540. <https://onlinelibrary.wiley.com/doi/abs/10.1111/2041-210X.12704>.
- Cai, Z., P. Jönsson, H. Jin, and L. Eklundh. 2017. “Performance of Smoothing Methods for Reconstructing NDVI Time-Series and Estimating Vegetation Phenology From MODIS Data.” *Remote Sensing* 9, no. 12: 1271. <https://www.mdpi.com/2072-4292/9/12/1271>.
- Capon, S. J., L. E. Chambers, R. Mac Nally, et al. 2013. “Riparian Ecosystems in the 21st Century: Hotspots for Climate Change Adaptation?” *Ecosystems* 16, no. 3: 359–381. <https://doi.org/10.1007/s10021-013-9656-1>.
- Carboneau, P., and H. Piégay. 2012. *Fluvial Remote Sensing for Science and Management*. Wiley Online Library.
- Chen, C., B. He, W. Yuan, L. Guo, and Y. Zhang. 2019. “Increasing Interannual Variability of Global Vegetation Greenness.” *Environmental Research Letters* 14, no. 12: 124005. <https://doi.org/10.1088/1748-9326/ab4ffc>.
- Chen, L., J.-G. Huang, Q. Ma, H. Hänninen, F. Tremblay, and Y. Bergeron. 2019. “Long-Term Changes in the Impacts of Global Warming on Leaf Phenology of Four Temperate Tree Species.” *Global Change Biology* 25, no. 3: 997–1004. <https://onlinelibrary.wiley.com/doi/abs/10.1111/gcb.14496>.
- Chen, T., R. A. M. de Jeu, Y. Y. Liu, G. R. van der Werf, and A. J. Dolman. 2014. “Using Satellite Based Soil Moisture to Quantify the Water Driven Variability in NDVI: A Case Study Over Mainland Australia.” *Remote Sensing of Environment* 140: 330–338. <https://www.sciencedirect.com/science/article/pii/S0034425713002800>.
- Chmielewski, F.-M., and T. Rötzer. 2001. “Response of Tree Phenology to Climate Change Across Europe.” *Agricultural and Forest Meteorology* 108, no. 2: 101–112. <https://www.sciencedirect.com/science/article/pii/S0168192301002337>.
- Choat, B., S. Jansen, T. J. Brodribb, et al. 2012. “Global Convergence in the Vulnerability of Forests to Drought.” *Nature* 491, no. 7426: 752–755. <https://www.nature.com/articles/nature11688>.
- Cornes, R. C., G. van der Schrier, E. J. M. van den Besselaar, and P. D. Jones. 2018. “An Ensemble Version of the E-OBS Temperature and Precipitation Data Sets.” *Journal of Geophysical Research: Atmospheres* 123, no. 17: 9391–9409. <https://onlinelibrary.wiley.com/doi/abs/10.1029/2017JD028200>.
- Daryaei, A., H. Sohrabi, C. Atzberger, and M. Immlitzer. 2020. “Fine-Scale Detection of Vegetation in Semi-Arid Mountainous Areas With Focus on Riparian Landscapes Using Sentinel-2 and UAV Data.” *Computers and Electronics in Agriculture* 177: 105686. <https://www.sciencedirect.com/science/article/pii/S0168169920312862>.
- de Jong, R., S. de Bruin, A. de Wit, M. E. Schaepman, and D. L. Dent. 2011. “Analysis of Monotonic Greening and Browning Trends From Global NDVI Time-Series.” *Remote Sensing of Environment* 115, no. 2: 692–702. <https://linkinghub.elsevier.com/retrieve/pii/S0034425710003160>.
- Dufour, S., and H. Piégay. 2008. “Geomorphological Controls of *Fraxinus excelsior* Growth and Regeneration in Floodplain Forests.” *Ecology* 89, no. 1: 205–215. <https://onlinelibrary.wiley.com/doi/abs/10.1890/06-1768.1>.
- Evans, D. G. Dritschel, and M. B. Singer. 2018. “Modeling Subsurface Hydrology in Floodplains.” *Water Resources Research* 54, no. 3: 1428–1459. <https://onlinelibrary.wiley.com/doi/abs/10.1002/2017WR020827>.
- Evans, L. M., S. Kaluthota, D. W. Pearce, et al. 2016. “Bud Phenology and Growth Are Subject to Divergent Selection Across a Latitudinal Gradient in *Populus angustifolia* and Impact Adaptation Across the Distributional Range and Associated Arthropods.” *Ecology and evolution* 6, no. 13: 4565–4581. <https://europepmc.org/articles/PMC4931002/>.
- Fruget, J.-F., and J. Dessaix. 2003. “Changements Environnementaux, d’Érives Biologiques et Perspectives de restauration du Rhône français après 200 ans d’influences anthropiques.” *VertigO - la revue électronique en sciences de l’environnement* 4, no. 3: 1–17. <http://journals.openedition.org/vertigo/3832>.
- Fu, B., and I. Burgher. 2015. “Riparian Vegetation NDVI Dynamics and Its Relationship With Climate, Surface Water and Groundwater.”

- Journal of Arid Environments* 113: 59–68. <https://www.sciencedirect.com/science/article/pii/S0140196314001943>.
- Fu, Y. H., S. Piao, N. Delpierre, et al. 2018. "Larger Temperature Response of Autumn Leaf Senescence Than Spring Leaf-Out Phenology." *Global Change Biology* 24, no. 5: 2159–2168. <https://onlinelibrary.wiley.com/doi/abs/10.1111/gcb.14021>.
- Fu, Y. H., S. Piao, M. Op de Beeck, et al. 2014. "Recent Spring Phenology Shifts in Western Central Europe Based on Multiscale Observations." *Global Ecology and Biogeography* 23, no. 11: 1255–1263. <https://onlinelibrary.wiley.com/doi/abs/10.1111/geb.12210>.
- Giorgi, F., and P. Lionello. 2008. "Climate Change Projections for the Mediterranean Region." *Global and Planetary Change* 63, no. 2: 90–104. <https://www.sciencedirect.com/science/article/pii/S092181807001750>.
- González, E., M. R. Felipe-Lucia, B. Bourgeois, et al. 2017. "Integrative Conservation of Riparian Zones." *Biological Conservation* 211: 20–29. <https://www.sciencedirect.com/science/article/pii/S0006320716306887>.
- Grossiord, C., S. Sevanto, H. D. Adams, et al. 2017. "Precipitation, Not Air Temperature, Drives Functional Responses of Trees in Semi-Arid Ecosystems." *Journal of Ecology* 105, no. 1: 163–175. <https://onlinelibrary.wiley.com/doi/abs/10.1111/1365-2745.12662>.
- Hashim, H., Z. Abd Latif, and N. A. Adnan. 2019. "Urban Vegetation Classification With NDVI Threshold Value Method With Very High Resolution (VHR) Pleiades Imagery." *International Archives of the Photogrammetry, Remote Sensing and Spatial Information Sciences* 42: 237–240. <https://isprs-archives.copernicus.org/articles/XLII-4-W16/237/2019/>.
- Henshaw, A. J., A. M. Gurnell, W. Bertoldi, and N. A. Drake. 2013. "An Assessment of the Degree to Which Landsat TM Data Can SUPPORT the assessment of Fluvial Dynamics, as Revealed by Changes in Vegetation Extent and Channel Position, Along a Large River." *Geomorphology* 202: 74–85. <https://www.sciencedirect.com/science/article/pii/S016955X1300038X>.
- Hew, C.-S., G. Krotkov, and D. T. Canvin. 1969. "Effects of Temperature on Photosynthesis and CO₂ Evolution in Light and Darkness by Green Leaves 1." *Plant Physiology* 44, no. 5: 671–677. <https://doi.org/10.1104/pp.44.5.671>.
- Huang, S., L. Tang, J. P. Hupy, Y. Wang, and G. Shao. 2021. "A Commentary Review on the Use of Normalized Difference Vegetation Index (NDVI) in the Era of Popular Remote Sensing." *Journal of Forestry Research* 32, no. 1: 1–6. <https://doi.org/10.1007/s11676-020-01155-1>.
- Hultine, K. R., R. Froend, D. Blasini, S. E. Bush, M. Karlinski, and D. F. Koepke. 2020. "Hydraulic Traits That Buffer Deep-Rooted Plants From Changes in Hydrology and Climate." *Hydrological Processes* 34, no. 2: 209–222. <https://onlinelibrary.wiley.com/doi/abs/10.1002/hyp.13587>.
- Huylebroeck, L., M. Laslier, S. Dufour, B. Georges, P. Lejeune, and A. Michez. 2020. "Using Remote Sensing to Characterize Riparian Vegetation: A Review of Available Tools and Perspectives for Managers." *Journal of Environmental Management* 267: 110652. <https://www.sciencedirect.com/science/article/pii/S0301479720305843>.
- Janssen, P., J. C. Stella, H. Piégay, et al. 2020. "Divergence of Riparian Forest Composition and Functional Traits From Natural Succession Along a Degraded River With Multiple Stressor Legacies." *Science of The Total Environment* 721: 137730. <http://www.sciencedirect.com/science/article/pii/S0048969720312419>.
- Kibler, C. L., E. C. Schmidt, D. A. Roberts, et al. 2021. "A Brown Wave of Riparian Woodland Mortality Following Groundwater Declines During the 2012–2019 California Drought." *Environmental Research Letters* 16, no. 8: 84030. <https://doi.org/10.1088/1748-9326/ac1377>.
- Kong, D., T. R. McVicar, M. Xiao, et al. 2022. "phenofit: An R Package for Extracting Vegetation Phenology From Time Series Remote Sensing." *Methods in Ecology and Evolution* 13, no. 7: 1508–1527. <https://onlinelibrary.wiley.com/doi/abs/10.1111/2041-210X.13870>.
- Li, J., and D. P. Roy. 2017. "A Global Analysis of Sentinel-2A, Sentinel-2B and Landsat-8 Data Revisit Intervals and Implications for Terrestrial Monitoring." *Remote Sensing* 9, no. 9: 902. <https://www.mdpi.com/2072-4292/9/9/902>.
- Lionello, P., P. Malanotte-Rizzoli, R. Boscolo, et al. 2006. "The Mediterranean Climate: An Overview of the Main Characteristics and Issues." In *Developments in Earth and Environmental Sciences*, edited by P. Lionello, P. Malanotte-Rizzoli, and R. Boscolo, Mediterranean, Vol. 4, 1–26. Elsevier. <https://www.sciencedirect.com/science/article/pii/S1571919706800030>.
- Liu, Y., Y. Li, S. Li, and S. Motesharrei. 2015. "Spatial and Temporal Patterns of Global NDVI Trends: Correlations with Climate and Human Factors." *Remote Sensing* 7, no. 10: 13233–13250. <https://www.mdpi.com/2072-4292/7/10/13233>.
- Lloret, F., A. Lobo, H. Estevan, P. Maisongrande, J. Vayreda, and J. Terradas. 2007. "Woody Plant Richness and NDVI Response to Drought Events in Catalonian (Northeastern Spain) Forests." *Ecology* 88, no. 9: 2270–2279.
- Lobo-do Vale, R., C. Kurz Besson, M. C. Caldeira, M. M. Chaves, and J. S. Pereira. 2019. "Drought Reduces Tree Growing Season Length but Increases Nitrogen Resorption Efficiency in a Mediterranean Ecosystem." *Biogeosciences* 16, no. 6: 1265–1279. <https://bg.copernicus.org/articles/16/1265/2019/>.
- Matzek, V., J. C. Stella, and P. Ropponen. 2018. "Development of a Carbon Calculator Tool for Riparian Forest Restoration." *Applied Vegetation Science* 21, no. 4: 584–594. <https://onlinelibrary.wiley.com/doi/abs/10.1111/avsc.12400>.
- Mavromatis, T., and D. Voulanas. 2021. "Evaluating ERA-Interim, Agri4Cast, and E-OBS Gridded Products in Reproducing Spatiotemporal Characteristics of Precipitation and Drought Over a Data Poor Region: The Case of Greece." *International Journal of Climatology* 41, no. 3: 2118–2136. <https://onlinelibrary.wiley.com/doi/abs/10.1002/joc.6950>.
- Mayes, M., K. K. Caylor, M. B. Singer, J. C. Stella, D. Roberts, and P. Nagler. 2020. "Climate Sensitivity of Water Use by Riparian Woodlands at Landscape Scales." *Hydrological Processes* 34, no. 25: 4884–4903. <https://onlinelibrary.wiley.com/doi/abs/10.1002/hyp.13942>.
- Mazerolle, M. J. 2020. "Model Selection and Multimodel Inference Using the AICcmodavg Package." R Vignette.
- McDowell, N. G., W. T. Pockman, C. D. Allen, et al. 2008. "Mechanisms of Plant Survival and Mortality During Drought: Why Do Some Plants Survive While Others Succumb to Drought?" *New Phytologist* 178, no. 4: 719–739. <https://onlinelibrary.wiley.com/doi/abs/10.1111/j.1469-8137.2008.02436.x>.
- Menzel, A., T. H. Sparks, N. Estrella, et al. 2006. "European Phenological Response to Climate Change Matches the Warming Pattern." *Global Change Biology* 12, no. 10: 1969–1976. <https://onlinelibrary.wiley.com/doi/abs/10.1111/j.1365-2486.2006.01193.x>.
- Merritt, D. M., M. L. Scott, N. Leroy Poff, G. T. Auble, and D. A. Lytle. 2010. "Theory, Methods and Tools for Determining Environmental Flows for Riparian Vegetation: Riparian Vegetation-Flow Response Guilds." *Freshwater Biology* 55, no. 1: 206–225. <https://onlinelibrary.wiley.com/doi/abs/10.1111/j.1365-2427.2009.02206.x>.
- Olivier, J.-M., G. Carrel, N. Lamouroux, et al. 2022. "Chapter 7 - The Rhône River Basin." In *Rivers of Europe (Second Edition)*, edited by K. Tockner, C. Zarfl, and C. T. Robinson, 391–451 en. Elsevier. <https://www.sciencedirect.com/science/article/pii/B9780081026120000079>.

- Osborne, J., and E. Waters. 2019. "Four Assumptions of Multiple Regression That Researchers Should Always Test." *Practical Assessment, Research, and Evaluation* 8, no. 1: 2. <https://scholarworks.umass.edu/pare/vol8/iss1/2>.
- Pace, G., C. Gutiérrez-Cánovas, R. Henriques, F. Boeing, F. Cássio, and C. Pascoal. 2021. "Remote Sensing Depicts Riparian Vegetation Responses to Water Stress in a Humid Atlantic Region." *Science of The Total Environment* 772: 145526. <https://www.sciencedirect.com/science/article/pii/S0048969721005945>.
- Palmer, M., C. A. Reidy Liermann, C. Nilsson, et al. 2008. "Climate Change and the World's River Basins: Anticipating Management Options." *Frontiers in Ecology and the Environment* 6, no. 2: 81–89. <https://onlinelibrary.wiley.com/doi/abs/10.1890/060148>.
- Pautou, G., J. Girel, and J.-L. Borel. 1992. "Initial Repercussions and Hydroelectric Developments in the French Upper Rhone Valley: A Lesson for Predictive Scenarios Propositions." *Environmental Management* 16, no. 2: 231–242. <https://doi.org/10.1007/BF02393828>.
- Peters, J. M. R., R. López, M. Nolf, et al. 2021. "Living on the Edge: A Continental-Scale Assessment of Forest Vulnerability to Drought." *Global Change Biology* 27, no. 15: 3620–3641. <https://onlinelibrary.wiley.com/doi/abs/10.1111/gcb.15641>.
- Pettit, N., and R. Froend. 2018. "How Important Is Groundwater Availability and Stream Perenniality to Riparian and Floodplain Tree Growth?" *Hydrological Processes* 32, no. 10: 1502–1514.
- Petts, G. E. 1989. "Historical Analysis of Fluvial Hydrosystems." In *Historical Change of Large Alluvial Rivers: Western Europe*, edited by G. E. Petts, H. Möller, and A. L. Roux, 1–18. Chichester: Wiley. <https://westminsterresearch.westminster.ac.uk/item/94w40/historical-analysis-of-fluvial-hydrosystems>.
- Piedallu, C., V. Chéret, J. P. Denux, et al. 2019. "Soil and Climate Differently Impact NDVI Patterns According to the Season and the Stand Type." *Science of The Total Environment* 651: 2874–2885. <https://www.sciencedirect.com/science/article/pii/S0048969718339251>.
- Piégay, H., F. Arnaud, B. Belletti, et al. 2020. "Remotely Sensed Rivers in the Anthropocene: State of the Art and Prospects." *Earth Surface Processes and Landforms* 45, no. 1: 157–188. <https://onlinelibrary.wiley.com/doi/abs/10.1002/esp.4787>.
- Puckridge, J. T., F. Sheldon, K. F. Walker, and A. J. Boulton. 1998. "Flow variability and the Ecology of Large Rivers." *Marine and Freshwater Research* 49, no. 1: 55–72. <https://www.publish.csiro.au/mf/mf94161>.
- Räpple, B. 2018. "Sedimentation Patterns and Riparian Vegetation Characteristics in Novel Ecosystems on the Rhône River, France : A Comparative Approach to Identify Drivers and Evaluate Ecological Potentials." (These de doctorat), Lyon. <https://www.theses.fr/2018YSEN006>.
- Riis, T., M. Kelly-Quinn, F. C. Aguiar, et al. 2020. "Global Overview of Ecosystem Services Provided by Riparian Vegetation." *BioScience* 70, no. 6: 501–514. <https://doi.org/10.1093/biosci/biaa041>.
- Rivaes, R., P. M. Rodríguez-González, A. Albuquerque, A. N. Pinheiro, G. Egger, and M. T. Ferreira. 2013. "Riparian Vegetation Responses to Altered Flow Regimes Driven by Climate Change in Mediterranean Rivers." *Ecohydrology* 6, no. 3: 413–424. <https://onlinelibrary.wiley.com/doi/abs/10.1002/eco.1287>.
- Rohde, M. M., J. C. Stella, D. A. Roberts, and M. B. Singer. 2021. "Groundwater Dependence of Riparian Woodlands and the Disrupting Effect of ANTHROPOGENICALLY ALTERED STREAMFLOW." *Proceedings of the National Academy of Sciences* 118, no. 25: e2026453118. <https://www.pnas.org/doi/abs/10.1073/pnas.2026453118>.
- Romano, G., G. F. Ricci, and F. Gentile. 2020. "Influence of Different Satellite Imagery on the Analysis of Riparian Leaf Density in a Mountain Stream." *Remote Sensing* 12, no. 20: 3376. <https://www.mdpi.com/2072-4292/12/20/3376>.
- Rood, S. B., S. G. Bigelow, and A. A. Hall. 2011. "Root Architecture of Riparian Trees: River Cut-Banks Provide Natural Hydraulic Excavation, Revealing That Cottonwoods Are Facultative Phreatophytes." *Trees* 25, no. 5: 907–917. <https://doi.org/10.1007/s00468-011-0565-7>.
- Sabathier, R., M. B. Singer, J. C. Stella, D. A. Roberts, and K. K. Taylor. 2021. "Vegetation Responses to Climatic and Geologic Controls on Water Availability in Southeastern Arizona." *Environmental Research Letters* 16, no. 6: 64029. <https://doi.org/10.1088/1748-9326/abfe8c>.
- Sargeant, C. I., and M. B. Singer. 2016. "Sub-Annual Variability in Historical Water Source Use by Mediterranean Riparian Trees." *Ecohydrology* 9, no. 7: 1328–1345. <https://onlinelibrary.wiley.com/doi/abs/10.1002/eco.1730>.
- Sargeant, C. I., and M. B. Singer. 2021. "Local and Non-Local Controls on Seasonal Variations in Water Availability and Use by Riparian Trees Along a Hydroclimatic Gradient." *Environmental Research Letters* 16, no. 8: 84018. <https://doi.org/10.1088/1748-9326/ac1294>.
- Sarris, D., D. Christodoulakis, and C. Körner. 2011. "Impact of Recent Climatic Change on Growth of Low Elevation Eastern Mediterranean Forest Trees." *Climatic Change* 106, no. 2: 203–223. <https://doi.org/10.1007/s10584-010-9901-y>.
- Sauquet, E., B. Richard, A. Devers, and C. Prudhomme. 2019. "Water Restrictions Under Climate Change: A Rhône–Mediterranean Perspective Combining Bottom-Up and Top-Down Approaches." *Hydrology and Earth System Sciences* 23, no. 9: 3683–3710. <https://hess.copernicus.org/articles/23/3683/2019/>.
- Schook, D. M., J. M. Friedman, C. A. Stricker, A. Z. Csank, and D. J. Cooper. 2020. "Short- and Long-Term Responses of Riparian Cottonwoods (*Populus* spp.) to Flow Diversion: Analysis of Tree-Ring Radial Growth and Stable Carbon Isotopes." *Science of The Total Environment* 735: 139523. <https://www.sciencedirect.com/science/article/pii/S0048969720330400>.
- Scott, M. L., P. B. Shafroth, and G. T. Auble. 1999. "Responses of Riparian Cottonwoods to Alluvial Water Table Declines." *Environmental Management* 23, no. 3: 347–358. <https://doi.org/10.1007/s002679900191>.
- Seavy, N., T. Gardali, G. Golet, et al. 2009. "Why Climate Change Makes Riparian Restoration More Important Than Ever: Recommendations for Practice and Research." *Ecological Restoration* 27: 330–338.
- Seignemartin, G., B. Mourier, J. Riquier, T. Winiarski, and H. Piégay. 2023. "Dike Fields as Drivers and Witnesses of Twentieth-Century Hydrosedimentary Changes in a Highly Engineered River (Rhône River, France)." *Geomorphology* 431: 108689. <https://www.sciencedirect.com/science/article/pii/S0169555X23001095>.
- Seneviratne, S. I., T. Corti, E. L. Davin, et al. 2010. "Investigating Soil Moisture–Climate Interactions in a Changing Climate: A Review." *Earth-Science Reviews* 99, no. 3: 125–161. <https://www.sciencedirect.com/science/article/pii/S0012825210000139>.
- Serrat-Capdevila, A., R. L. Scott, W. James Shuttleworth, and J. B. Valdés. 2011. "Estimating Evapotranspiration Under Warmer Climates: Insights From a Semi-Arid Riparian System." *Journal of Hydrology* 399, no. 1: 1–11. <https://www.sciencedirect.com/science/article/pii/S0022169410007869>.
- Singer, M. B., C. I. Sargeant, H. Piégay, J. Riquier, R. J. S. Wilson, and C. M. Evans. 2014. "Floodplain Ecohydrology: Climatic, Anthropogenic, and Local Physical Controls on Partitioning of Water Sources to Riparian Trees." *Water Resources Research* 50, no. 5: 4490–4513. <https://agupubs.onlinelibrary.wiley.com/doi/abs/10.1002/2014WR015581>.
- Singer, M. B., J. C. Stella, S. Dufour, H. Piégay, R. J. S. Wilson, and L. Johnstone. 2013. "Contrasting Water-Uptake and Growth Responses to Drought in Co-Occurring Riparian Tree Species." *Ecohydrology* 6, no. 3: 402–412. <https://onlinelibrary.wiley.com/doi/10.1002/eco.1283>.
- Stella, J. C., and J. J. Battles. 2010. "How do Riparian Woody Seedlings Survive Seasonal Drought?." *Oecologia* 164, no. 3: 579–590. <https://doi.org/10.1007/s00442-010-1657-6>.

- Stella, J. C., J. Riddle, H. Piégay, M. Gagnage, and M.-L. Trémélo. 2013. "Climate and Local Geomorphic Interactions Drive Patterns of Riparian Forest Decline Along a Mediterranean Basin River." *Geomorphology* 202: 101–114. <https://www.sciencedirect.com/science/article/pii/S016955X13000500>.
- Stella, J. C., P. M. Rodríguez-González, S. Dufour, and J. Bendix. 2013. "Riparian Vegetation Research in Mediterranean-Climate Regions: Common Patterns, Ecological Processes, and Considerations for Management." *Hydrobiologia* 719: 291–315.
- Tai, X., D. S. Mackay, J. S. Sperry, et al. 2018. "Distributed Plant Hydraulic and Hydrological Modeling to Understand the Susceptibility of Riparian Woodland Trees to Drought-Induced Mortality." *Water Resources Research* 54, no. 7: 4901–4915. <https://onlinelibrary.wiley.com/doi/abs/10.1029/2018WR022801>.
- Taufik, A., S. S. Syed Ahmad, and E. F. Azmi. 2019. "Classification of Landsat 8 Satellite Data Using Unsupervised Methods." In *Intelligent and Interactive Computing*, edited by V. Piuri, V. E. Balas, S. Borah, and S. S. Syed Ahmad, 275–284. Singapore: Springer.
- Team, R. C. 2022. "R: A Language and Environment for Statistical Computing. R Foundation for Statistical Computing, Vienna, Austria." <https://www.R-project.org/>.
- Tonkin, J. D., D. M. Merritt, J. D. Olden, L. V. Reynolds, and D. A. Lytle. 2018. "Flow Regime Alteration Degrades Ecological Networks in Riparian Ecosystems." *Nature Ecology & Evolution* 2, no. 1: 86–93. <https://www.nature.com/articles/s41559-017-0379-0>.
- Vicente-Serrano, S. M., C. Gouveia, J. J. Camarero, et al. 2013. "Response of Vegetation to Drought Time-Scales Across Global Land Biomes." *Proceedings of the National Academy of Sciences* 110, no. 1: 52–57. <https://www.pnas.org/doi/abs/10.1073/pnas.1207068110>.
- Vitasse, Y., A. J. Porté, A. Kremer, R. Michalet, and S. Delzon. 2009. "Responses of Canopy Duration to Temperature Changes in Four Temperate Tree Species: Relative Contributions of Spring and Autumn Leaf Phenology." *Oecologia* 161, no. 1: 187–198. <http://link.springer.com/10.1007/s00442-009-1363-4>.
- Vivian, H. 1989. "Hydrological Changes of the Rhône River." *Hydrological Changes of the Rhône River*: 57–77. Num Pages: 21 Place: Chichester Publisher: John Wiley.
- Walker, D. A., H. E. Epstein, G. J. Jia, et al. 2003. "Phytomass, LAI, and NDVI in Northern Alaska: Relationships to Summer Warmth, Soil pH, Plant Functional Types, and Extrapolation to the Circumpolar Arctic." *Journal of Geophysical Research: Atmospheres* 108, no. D2: 8169. <https://onlinelibrary.wiley.com/doi/abs/10.1029/2001JD000986>.
- Wang, J., P. M. Rich, and K. P. Price. 2003. "Temporal Responses of NDVI to Precipitation and Temperature in the Central Great Plains, USA." *International Journal of Remote Sensing* 24, no. 11: 2345–2364. <https://doi.org/10.1080/01431160210154812>.
- Wang, R., J. A. Gamon, R. A. Montgomery, et al. 2016. "Seasonal Variation in the NDVI–Species Richness Relationship in a Prairie Grassland Experiment (Cedar Creek)." *Remote Sensing* 8, no. 2: 128. <https://www.mdpi.com/2072-4292/8/2/128>.
- Wang, S. Adiku, J. Tenhunen, and A. Granier. 2005. "On the Relationship of NDVI With Leaf Area Index in a Deciduous Forest Site." *Remote Sensing of Environment* 94, no. 2: 244–255. <https://www.sciencedirect.com/science/article/pii/S034425704003232>.
- Warter, M. M., M. B. Singer, M. O. Cuthbert, et al. 2023. "Modeling Seasonal Vegetation Phenology From Hydroclimatic Drivers for Contrasting Plant Functional Groups Within Drylands of the Southwestern USA." *Environmental Research: Ecology* 2, no. 2: 25001. <https://doi.org/10.1088/2752-664X/acb9a0>.
- Williams, J., J. C. Stella, S. L. Voelker, et al. 2022. "Local Groundwater Decline Exacerbates Response of Dryland Riparian Woodlands to Climatic Drought." *Global Change Biology* 28, no. 22: 6771–6788. <https://onlinelibrary.wiley.com/doi/abs/10.1111/gcb.16376>.
- Yang, G., H. Shen, L. Zhang, Z. He, and X. Li. 2015. "A Moving Weighted Harmonic Analysis Method for Reconstructing High-Quality SPOT VEGETATION NDVI Time-Series Data." *IEEE Transactions on Geoscience and Remote Sensing* 53, no. 11: 6008–6021. <https://ieeexplore.ieee.org/document/7116551>.
- Yao, J., Y. Chen, Y. Zhao, et al. 2018. "Response of Vegetation NDVI to Climatic Extremes in the Arid Region of Central Asia: A Case Study in Xinjiang, China." *Theoretical and Applied Climatology* 131, no. 3: 1503–1515. <https://doi.org/10.1007/s00704-017-2058-0>.
- Yin, F., P. E. Lewis, J. L. Gomez-Dans, and Q. Wu. 2019. "A Sensor-Invariant Atmospheric Correction Method: Application to Sentinel-2/MSI and Landsat 8/OLI." <https://eartharxiv.org/repository/view/1034/>.
- Zhang, K., J. S. Kimball, R. R. Nemani, et al. 2015. "Vegetation Greening and Climate Change Promote Multidecadal Rises of Global Land Evapotranspiration." *Scientific Reports* 5, no. 1: 15956. <https://www.nature.com/articles/srep15956>.

Supporting Information

Additional supporting information can be found online in the Supporting Information section.